Intra-atomic photoluminescence at 1.41 eV of substitutional Mn in GaMnN of high optical quality

J. Zenneck, T. Niermann, D. Mai, M. Roever, M. Kocan, J. Malindretos, M. Seibt, A. Rizzi, N. Kaluza, and H. Hardtdegen

Citation: Journal of Applied Physics **101**, 063504 (2007);
View online: https://doi.org/10.1063/1.2710342
View Table of Contents: http://aip.scitation.org/toc/jap/101/6
Published by the American Institute of Physics

Intra-atomic photoluminescence at 1.41 eV of substitutional Mn in GaMnN of high optical quality

J. Zenneck,[a] T. Niermann, D. Mai, M. Roever, M. Kocan, J. Malindretos, M. Seibt, and A. Rizzi
IV. Physikalisches Institut and Virtual Institute of Spin Electronics (VISel), Georg-August Universität Göttingen, D-37077 Göttingen, Germany

N. Kaluza and H. Hardtdegen
Institute of Bio- and Nanosystems (IBN-1), Center of Nanoelectronic Systems for Information Technology (CNI), Virtual Institute of Spin Electronics (VISel), Research Center Juelich, D-52425 Juelich, Germany

(Received 22 December 2006; accepted 11 January 2007; published online 16 March 2007)

We report on a characteristic photoluminescence feature of the substitutional Mn in high quality GaMnN layers. The lattice site was identified using atom localization by channeling enhanced microanalysis with a transmission electron microscope. It shows that 96.5%±5.0% of the Mn atoms are incorporated on the substitutional Ga site. In photoluminescence a feature appears at 1.41 eV with a phonon sideband related to the GaN matrix. The temperature evolution is characteristic of an intra-atomic transition and it is assigned to the internal transition $^5E \rightarrow {}^5T_2$ of the Mn^{3+} ion. The assignment is supported by absorption experiments. The persistence of the clear PL signal up to about 1% Mn concentration is proposed to be a fingerprint of high quality diluted GaMnN. © *2007 American Institute of Physics*. [DOI: 10.1063/1.2710342]

Diluted magnetic semiconductors on the basis of III-V compounds have received major attention over the past years. Early calculations predicted room temperature ferromagnetic behavior for GaMnN, bringing the focus to this material system.[1] On the other hand recent first-principles calculations taking into account the short range character of the double exchange interaction deny the room temperature ferromagnetism.[2] Experimentally ferromagnetism with widely varying Curie temperatures as well as spin-glass behavior have been observed in single phase GaMnN.[3]

To achieve a consistent explanation of the experimental results and draw conclusions about the application potential of GaMnN as a room temperature spin polarized semiconductor, some benchmarks have to be established to classify the material properties of different samples. Optical measurements are an invaluable tool for probing the electronic structure and indeed several Mn-related transitions have been identified in absorption, in particular, an internal transition of the Mn^{3+} ion at 1.42 eV and a broad feature above 1.8 eV related to a transition from the valence band.[4] The same internal transition has recently been observed by cathodoluminescence (CL) (Ref. 5) but could not be detected in photoluminescence (PL) up to now, not even at Mn concentrations below 1%. For structural characterization transmission electron microscopy (TEM) is a powerful and widely available tool, which can even yield information about the lattice site.

In this work we present a study relating PL measurements with TEM characterization and comparing them with available experimental and theoretical data, mainly the known absorption features. We show that if the incorporation of the Mn in GaN is to a very high degree substitutional, then a clear PL at 1.41 eV is detected. Furthermore also an intense band edge PL is measured, comparable to the one in the host material. Above 1% Mn concentration both features are continuously quenched.

The GaMnN-samples are grown by plasma-assisted molecular beam epitaxy (MBE) at various temperatures as described in Ref. 6. They are grown either on *p*-doped Si(111) with an AlN buffer layer or on top of a metal-organic chemical-vapor deposition (MOCVD)-grown GaN template on Si(111) or sapphire. PL measurements were carried out with the 325 nm line of a HeCd laser typically at a power of 100 W/cm^2. For low temperature spectra the samples were kept in a liquid helium immersion cryostat at 2 K and dispersed by a 0.75 m Acton monochromator with a charge-coupled device (CCD) camera. Transmission electron microscopy (TEM) and energy dispersive x-ray (EDX) measurements were carried out using a Philips CM 200 UT-FEG operated at 200 keV. The microscope is equipped with a Si:Li detector (Oxford Link ISIS) for EDX analysis. The samples show only a single phase in x-ray diffraction (XRD) and TEM.

In order to quantitatively determine the fraction of Mn atoms on substitutional and interstitial sites, atom localization by channeling enhanced microanalysis (ALCHEMI) was carried out in the TEM. The basic idea of this technique is to exploit the strong dependence of the characteristic x-ray emission on small changes of the crystal orientation due to changes of the dynamical diffraction conditions.[7] Soo *et al.* [extended x-ray-absorption fine structure (EXAFS)[8]] and Kuroda *et al.* [angular-resolved particle-induced x-ray emission (PIXE)][9] already showed the substitutional incorporation, but they used integral methods while the method presented here is locally applied on defect-free areas. Structural

[a]Electronic mail: zenneck@ph4.physik.uni-goettingen.de

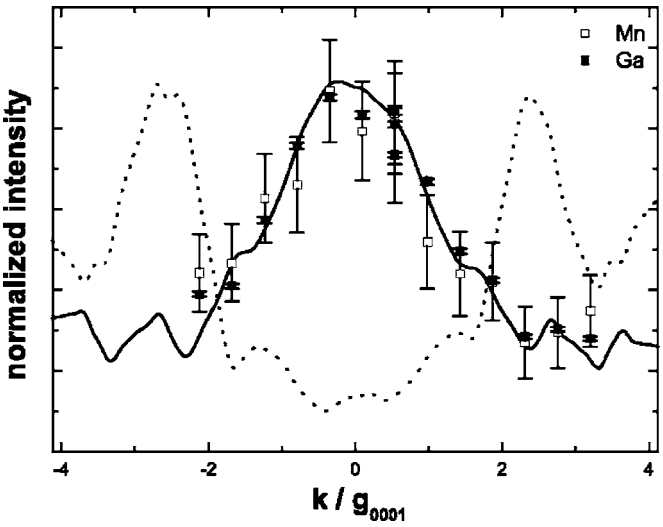

FIG. 1. Measured (squares with error bars) and calculated x-ray intensities for ALCHEMI using a systematic row of {0002} reflections. The solid line shows the calculation for the cation site of GaN, the dotted line for the interstitial sites.

defects may influence the results of angular-resolved measurements and can thus be avoided by ALCHEMI.

For the analysis we considered substitutional Mn on the cation site of the GaN host matrix as well as on the octahedral (O) and tetrahedral (T) interstitial sites. Planar channeling conditions with a systematic row of {0002} reflections allow us to differentiate between the interstitial and substitutional sites, while a further differentiation between the two interstitial sites under consideration is not possible. In addition, measurements using a row of $\{11\bar{2}0\}$ reflections were carried out.

The measured total Mn concentration of the sample studied by ALCHEMI is about 1.5% of the metal content. We used Bloch wave calculations to simulate the thickness integrated electron density on all possible sites using the EMS software package.[10] In the absence of delocalization effects this density can be assumed to be proportional to the emitted x-ray signal. The calculated signals for all considered sites are compared to the experimentally obtained ones.[11]

Figure 1 shows the measured K_α intensity of the Ga and Mn signal for different incident beam angles along the row of {0002} reflections. The calculated intensities for the cation and interstitial site are also plotted. The occupancy analysis itself was done by matching a linear combination of the calculated Mn/Ga ratios for substitutional and interstitial sites to the ratio of the measured lines. Analyzing the ratios is common in quantitative EDX analysis,[12] as it allows us to minimize the influence of experimental uncertainties as, e.g., changes in the electron intensity. This analysis revealed that 96.5%±5.0% of the Mn atoms are located on the substitutional Ga site. The error of the occupancy was obtained by a Monte Carlo simulation using the Poisson's statistics of the absolute count rates. We were able to reproduce this result within the error examining other regions of the sample. These results were cross checked with a measurement along a row of $\{11\bar{2}0\}$ reflections (not shown), which allows to exclude Mn locations besides those considered above.

With the quantitative knowledge of the lattice site occupation in our samples we can now analyze the optical properties of GaMnN. As compared with undoped GaN, the incorporation of Mn leads to a new band at 1.41 eV, which shifts slightly with strain on different substrates. When the Mn-concentration increases above 1 at. %, we can detect nearly no luminescence from the sample at all.

Details of the luminescence band in the infrared (IR) region are shown in Fig. 2. The electronic 3d-levels of a manganese atom located at the gallium site are split by the approximate tetrahedral symmetry of the crystal field of the ligands into a doubly degenerate *e* state and a triply degenerate t_2 state. The t_2 orbitals further hybridize with the *p*-like orbitals of the nitrogen neighbors forming bonding states inside the valence band and antibonding states above the nonbonding *e* states. Density-functional theory predicts an energy difference between the antibonding t_2 states and the *e* states of approximately 1.4 eV for Mn^{3+}.[13] The ground state of a free Mn^{3+} ion with its four *d* electrons is ^5D. The crystal field splitting of the *d* orbitals splits this state into the new ground state $^5T_2$ where the hole is located in the t_2 levels and an excited state ^5E where the hole is located in the *e* levels.

A (spin-allowed) transition from the excited state ^5E to the ground state $^5T_2$ inside the Mn^{3+} ion is then assigned to the observed luminescence (Fig. 2). Below the zero-phonon line (ZPL), a structured sideband of phonon replica is visible.

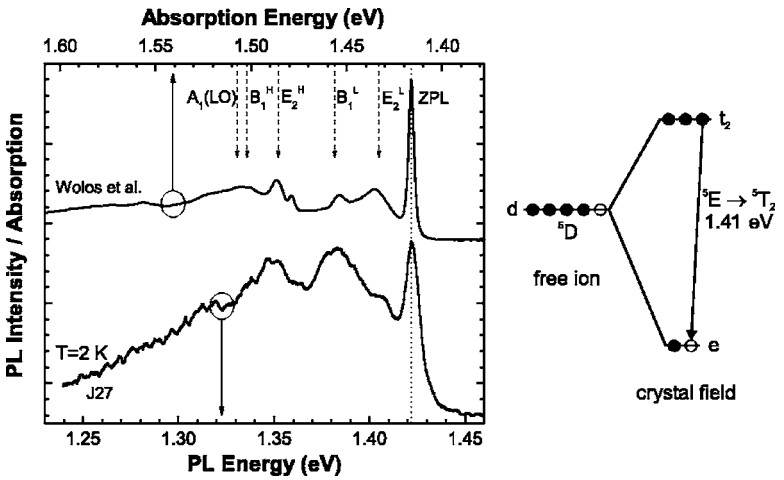

FIG. 2. Details of the IR luminescence band of a GaMnN layer grown at 760 °C on Si(111) with a Mn content of about 0.5% (lower spectrum). The upper spectrum shows the absorption data from Ref. 14 with an inverted energy scale (courtesy of A. Wolos). The proposed transition is shown on the right.

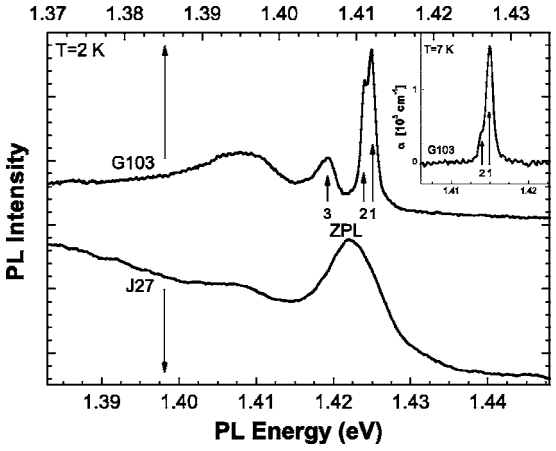

FIG. 3. Comparison between a sample grown on Si(111) (J27) and on a MOCVD-template on sapphire (G103) with comparable Mn concentration (~0.5%). The inset shows an absorption measurement.

Figure 2 also shows absorption data from Wolos *et al.*[14] with qualitatively the same features as our luminescence data. These absorption features are commonly found in GaMnN[4,5,14] and identified by Graf *et al.*[4] as the internal transition $^5T_2 \rightarrow {}^5E$ of the neutral acceptor (A^0) Mn^{3+}. The good agreement of the sideband with phonon modes in GaN has been pointed out by Wolos *et al.*[14] and are marked in Fig. 2.

In Fig. 3 a comparison between GaMnN grown on different substrates is shown. The Mn concentration amounts to approximately 0.5%. The optical quality is much better in the samples grown on sapphire. These layers also show a remarkably improved crystal quality in XRD and TEM. Furthermore, PL near the band edge (not shown) reveals very strong bound and free excitonic signals with a FWHM of 2–3 meV, which is identical to that of the MOCVD layer. Three zero-phonon lines near 1.4 eV are well resolved which can be explained by crystal-field theory taking into account trigonal components and spin-orbit coupling as shown by Marcet *et al.*[5] ZPL 1 and 2 are seperated by 1 meV through spin-orbit coupling, while ZPL 3 is 6 meV apart from ZPL 1 because of the trigonal field. After[5] a spin-orbit triplet is expected, but two of the lines merge into ZPL 1. In absorption measurements a doublet can be resolved showing the ZPLs 1 and 2 (Fig. 3 inset). Another significant difference between the two sets of samples is the strength of the phonon sideband, which is much weaker for the samples grown on sapphire. Other groups were not able to detect the above intra-3D luminescence in PL but only with CL in one very diluted sample and at very high excitation densities.[5]

The temperature dependence of the Mn-related band at 1.41 eV (not shown) is typical for an intra-atomic transition. The sharp ZPL weakens with increasing temperature and around 100 K becomes indistinguishable from the broad band at lower energy. It should be noted that the intensity of the Mn-related band at 1.41 eV does not scale proportional to the Mn concentration in the layer. We find a decreasing intensity for highly concentrated samples. Indeed, the whole luminescence over the full spectral range quenches with increasing Mn concentration, indicating the creation of nonradiative recombination channels competing with the radiative processes. Also we find a correlation between the existence of the PL at 1.41 eV and the existence of the excitonic luminescence near the band edge. This is an indication that the excitation mechanism involves excitons, which is further supported by our inability to detect the PL with below bandgap excitation. An Auger-like energy transfer to the Mn atom fulfills these requirements and is thus proposed as the excitation mechanism.

In conclusion, we report on the first observation of the intra-atomic transition $^5E \rightarrow {}^5T_2$ of substitutional Mn in GaMnN in photoluminescence. The analysis by ALCHEMI revealed that 96.5%±5.0% of the Mn atoms in our samples are located on the substitutional Ga site. The PL line shape and intensity are highly sensitive to the structural properties of the grown layers. The appearance of this feature now opens up further possibilities to analyze the electronic structure of Mn^{3+} in GaMnN, e.g., via magneto-optical experiments.

This research was partially supported by the Deutsche Forschungsgemeinschaft (SFB 602). The authors thank W. Pacuski and D. Ferrand of the LSP Grenoble for the collaboration on absorption measurements. A. Dadgar is acknowledged for kindly providing GaN templates on Si(111) and R. G. Ulbrich for fruitful discussions.

[1] T. Dietl, H. Ohno, F. M. J. Cibert, and D. Ferrand, Science **287**, 1019 (2000).
[2] K. Sato, P. Dederichs, and H. Katayama-Yoshida, Physica B **376**, 639 (2006).
[3] C. Liu, F. Yun, and H. Morkoc J. Mater. Sci.: Mater. Electron. **16**, 555 (2005).
[4] T. Graf, M. Gjukic, M. S. Brandt, M. Stutzmann, and O. Ambacher, Appl. Phys. Lett. **81**, 5159 (2002).
[5] S. Marcet, D. Ferrand, D. Halley, S. Kuroda, H. Mariette, E. Gheeraert, F. Teran, M. Sadowski, R. M. Galera, and J. Cibert, Phys. Rev. B **74**, 125201 (2006).
[6] M. Kocan, J. Malindretos, M. Roever, J. Zenneck, T. Niermann, D. Mai, M. Bertelli, M. Seibt, and A. Rizzi Semicond. Sci. Technol. **21**, 1348 (2006).
[7] I. Jones, Adv. Imaging Electron Phys. **125**, 63 (2002).
[8] Y. L. Soo, G. Kioseoglou, S. Kim, S. Huang, Y. H. Kao, S. Kuwabara, S. Owa, T. Kondo, and H. Munekata, Appl. Phys. Lett. **79**, 3926 (2001).
[9] S. Kuroda, S. Marcet, E. Bellet-Amalric, J. Cibert, H. Mariette, S. Yamamoto, T. Sakai, T. Ohshima, and H. Itoh, Phys. Status Solidi A **203**, 1724 (2006)
[10] P. A. Stadelmann, Ultramicroscopy **21**, 131 (1987).
[11] L. J. Allen, T. W. Josefsson, and C. J. Rossouw, Ultramicroscopy **55**, 258 (1994).
[12] G. Cliff and G. W. Lorimer, J. Microsc. **103**, 203 (1975).
[13] Z. S. Popovic, S. Satpathy, and W. Mitchel, Phys. Rev. B **70**, 161308 (2004).
[14] A. Wolos, A. Wysmolek, M. Kaminska, A. Twardowski, M. Bockowski, I. Grzegory, S. Porowski, and M. Potemski, Phys. Rev. B **70**, 245202 (2004).